Journal of the European Ceramic Society **18** (1998) 1629–1635
© 1998 Elsevier Science Limited
Printed in Great Britain. All rights reserved
PII: S0955-2219(98)00029-6
0955-2219/98/$—see front matter

Dielectric Relaxation Behaviour of Bi:SrTiO$_3$: III. Dielectric Properties in the Temperature Range of 300–600 K

Yu Zhi, Ang Chen,* P. M. Vilarinho, P. Q. Mantas and J. L. Baptista†

Department of Ceramics and Glass Engineering, University of Aveiro, Aveiro, Portugal

(Received 1 July 1997; accepted 2 February 1998)

Abstract

$(Sr_{1-1.5x}Bi_x)TiO_3$ ceramics show several polarisation and conduction mechanisms in different temperature ranges. In the present paper, the permittivity peaks that occurred in the temperature range from 300 to 600 K are discussed for the samples both as-sintered and O_2 or N_2 annealed. The activation energy for conduction in the temperature range in which these permittivity peaks occurred is around 0·59–0·78 eV. This suggests that the carriers responsible for the conduction are coming from the thermal excitation of electrons from the $V_o^{\bullet}$ state to the conduction band. The activation energy for dielectric relaxation is in the range of 0·64–0·86 eV. The discussion on the correlation between dielectric relaxation and conduction, led to suggest that the permittivity peaks are related to a dipole-like dielectric relaxation either for the as-sintered samples aswell as for the ones annealed in O_2. However, for the samples annealed in N_2, the results indicate that the polarisation mechanism is related to the trap-controlled ac conduction. © 1998 Elsevier Science Limited. All rights reserved

1 Introduction

Interesting properties of SrTiO$_3$ based materials have attracted much attention both from the theoretical as well as from the technical points of view.[1–4] Especially, the dielectric and the electrical properties of impurity doped SrTiO$_3$ have been extensively studied[5–8] because of their wide applications in electronic industry.[9–11] By systematically studying the dielectric properties of the (Sr$_{1-1.5x}$Bi$_x$)TiO$_3$ solid solution, in a wide temperature range, the present authors have reported the existence of several sets of permittivity peaks with frequency dispersion. For example, for $x = 0{\cdot}0267$, at 1 KHz, besides the permittivity peaks around 100 K reported by Skanavi *et al.*,[12,13] there are a second set of permittivity peaks around 210 K, which can be eliminated by annealing in oxygen,[14] a third set around 410 K, and a fourth set around 620 K. In the previous papers, the first (lower than 200 K) and the second peak (200–300 K) and the influence of the annealing atmosphere on the dielectric relaxation of the (Sr$_{1-1.5x}$Bi$_x$)TiO$_3$ solid solutions containing lower Bi concentrations were reported and discussed.[14,15]

The present paper is mainly concerned with the dielectric properties of the third set of peaks, i.e. the one in the temperature range 300–600 K, and the influence of heat treatments on the dielectric properties of the (Sr$_{1-1.5x}$Bi$_x$)TiO$_3$ ceramics.

2 Experimental Procedure

The ceramic samples of (Sr$_{1-1.5x}$Bi$_x$)TiO$_3$ ($x = 0{\cdot}0267$, 0·04, 0·0533, 0·08, 0·10, 0·133) were prepared by solid state reaction as described in Part I.

The temperature dependence of dielectric properties and resistance was measured from 300 to 600 K in a frequency range from 1 Hz to 1 MHz. The detailed procedure was also described in Parts I and II.

---

*Permanent address: Department of Physics, Zhejiang University, Hangzhou 310027, People's Republic of China.

†To whom correspondence should be addressed. Fax; 00351 34 25300

3 Results

3.1 Dielectric relaxation behaviour

3.1.1 Influence of Bi concentration on relaxation at high temperatures

The temperature dependence of the permittivity (ε) and dissipation factor ($\tan\delta$) in the temperature range 300–600 K, for the samples with $x = 0{\cdot}0267$, 0·04, 0·0533, 0·08, 0·10 and 0·133 at 1 kHz are shown in Fig. 1. A set of permittivity and dissipation factor peaks can be seen. The temperature range where the peaks occurred is shown in Table 1. At temperature higher than 550 K, the peaks are covered by the fast increase of ε and $\tan\delta$ with temperature.

The dependence of the temperature of permittivity maximum (T_m) is shown in Fig. 2. It shows that with increase in Bi concentration, the T_m slightly increases.

The temperature dependence of permittivity and dissipation factor at several frequencies for the samples with $x = 0{\cdot}0267$, 0·04, 0·0533 and 0·10 is shown in Figs 3–6, respectively. It can be seen that both permittivity and dissipation factor peaks are frequency dependent. With the increase in frequency, the permittivity maximum as well as the maximum of the dissipation factor are shifted to higher temperatures.

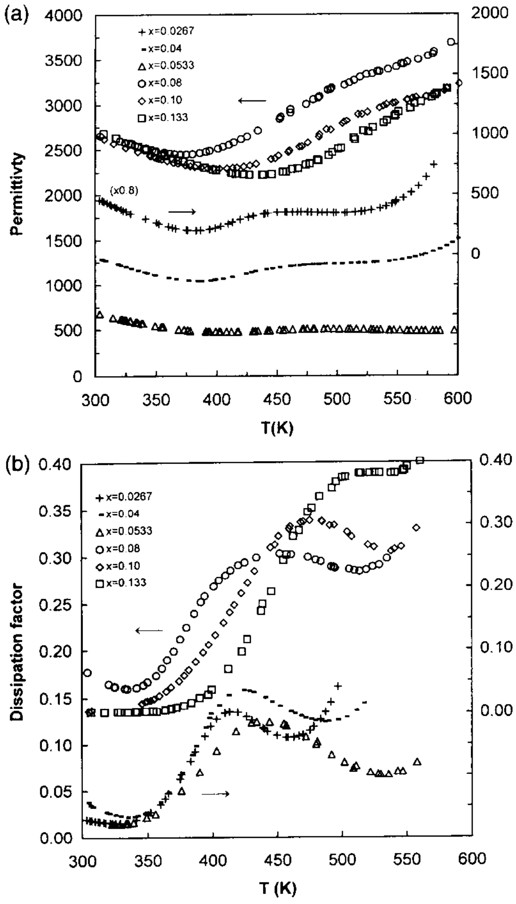

Fig. 1. Temperature dependence of (a) the permittivity and (b) the dissipation factor for $x = 0{\cdot}0267$, 0·04, 0·0533, 0·08, 0·10, 0·1330 at 1 kHz. (Note: the label in the bracket is the magnification scale.)

At 430 K, the frequency dependence of permittivity and dissipation factor for $x = 0{\cdot}0267$ 0·0533 and 0·010 is shown in Fig. 7. From 1 to 10^6 Hz, the permittivity decreases with the increase in frequency and the peak of the dissipation factor occurred at 5×10^3 Hz and 1.5×10^2 Hz for $x = 0{\cdot}0267$ and 0·0533, respectively. The relaxation time was estimated to be 2×10^{-4} s for $x = 0{\cdot}0267$, and 7×10^{-3} s for $x = 0{\cdot}0533$. A similar profile of frequency dependence was found for all the samples. Moreover, the dissipation peak is shifted to lower frequencies with the increase in the bismuth content; this is in agreement with the increase of the temperature of the maximum of $\tan\delta$ with the increase in Bi content.

3.1.2 Dielectric relaxation time and activation energy

Figures 3–6 show that dielectric permittivity peaks with obvious frequency dispersion occurred in the temperature range 300–600 K. The profile of the dissipation loss peaks seems however to deviate from the Debye model. As was done in Part II, a modified Debye equation is adopted to evaluate the relaxation.[16]

$$\varepsilon^* = \varepsilon_\infty + (\varepsilon_0 - \varepsilon_\infty)/[1 + (i\omega\tau)^\beta] \qquad (1)$$

Samples were fitted to the experimental data using eqn (1) with the least square approach. Typical results, for instance for $x = 0{\cdot}0533$ annealed in O_2 are shown in Fig. 8. The parameter β is in the range 0·46–0·54.

As described in Part II, the relaxation time can also be calculated from the modified Debye equation at various temperatures. The relaxation time τ as a function of the inverse of absolute temperature ($1/T$) for various frequencies is shown in Fig. 9. It is clear that a linear relation between $\log\tau$ and $1/T$ is obtained in the temperature range 403 to 544 K. The relaxation time also obeys the Ahrrenius law:

$$\tau = \tau_0 \exp(E_{\mathrm{relax}}/k_B T)$$

A straight line fitting to Arrhenius law gave the activation energy for relaxation $E_{\mathrm{relax}} = 0{\cdot}81\ eV$ and $\tau_0 = 1\times10^{-13}$ s.

The activation energies (E_{relax}) of the dielectric relaxation for other samples, $x = 0{\cdot}0267$, 0·04, 0·0533 (as-sintered and annealed in N_2) and 0·10 (as-sintered and annealed in N_2) obtained by

Table 1. Activation energy, temperature regime in which permittivity peak occurred (at 1 kHz) of the samples as-sintered and annealed in O$_2$ and N$_2$

x	*0·0267*	*0·04*	*0·0533*	*0·0533 (annealed in O$_2$)*	*0·0533 (annealed in N$_2$)*	*0·10 (as-sintered)*	*0·10 (annealed in N$_2$)*
E_{relax} (eV)	0·74	0·77	0·82	0·76	0·64	0·86	0·64
Temperature range (K)	350–460	360–470	350–510	350–500	350–600	350–600	350–650
E_{cond} (eV)	0·59	0·68	0·76	—	0·63	0·78	0·66

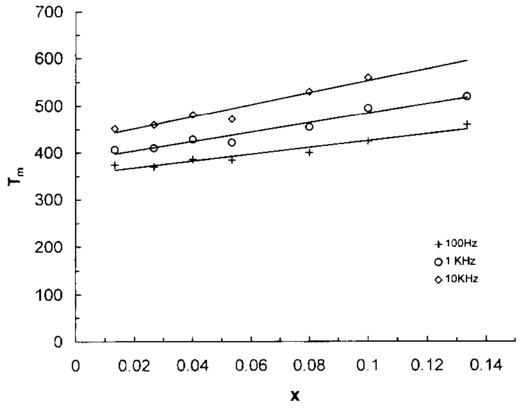

Fig. 2. The concentrational dependence of temperature of the permittivity maximum T_m at 1, 10 and 100 kHz.

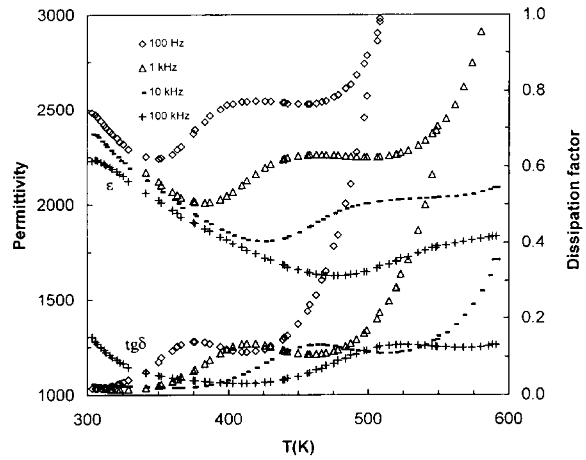

Fig. 4. Temperature and frequency dependence of permittivity and dissipation factor for the as-sintered sample with $x = 0·04$.

similar fitting, are listed in Table 1. The activation energies varied between 0·74–0·86 eV.

3.1.3 Dielectric properties of the annealed samples

As previously described in Part II, it was noted that post sintering heat treatments carried out under controlled atmosphere were also affecting the high temperature dielectric properties here described.

Figure 5(b) shows the effect of oxygen annealing (800°C, 40 h) on the dielectric properties of the $x = 0·0533$ sample. It can be seen that, both the permittivity and the dissipation factor decreased, and that the resistivity increased while the colour of the sample was becoming lighter. On the contrary, the permittivity is greatly enhanced and the maxima of the dissipation factor peaks increased as well when the same sample was annealed in nitrogen atmosphere, as shown in Fig. 5(c). Similar increase in permittivity and dissipation factor for the nitrogen annealed sample with $x = 0·10$ is shown in Fig. 6(b). These results indicated that the dielectric properties are closely related to an oxidation-reduction process, possibly involving variations in the concentration of oxygen vacancies in the samples.

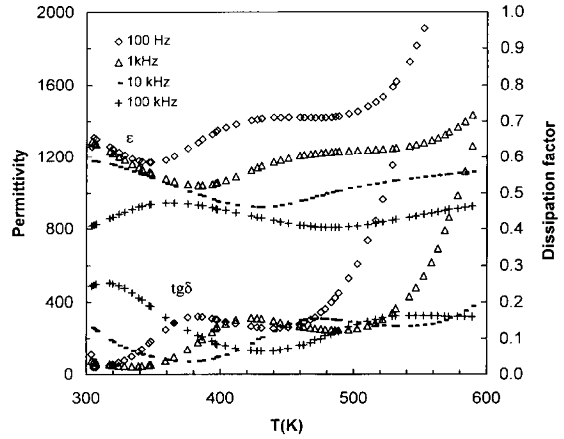

Fig. 3. Temperature and frequency dependence of permittivity and dissipation factor for the as-sintered sample with $x = 0·0267$.

The activation energy of the samples annealed in O$_2$ and N$_2$, were calculated in the same way as described above (Figs 8 and 9); the values are listed in Table 1.

3.2 Temperature dependence of conductivity

The plots of dc conductivity versus inverse absolute temperature ($1/T$) of the as-sintered sample with $x = 0·0267$, 0·04, 0·0533 and 0·10 are shown in Fig. 10(a). The relation between $\log\sigma$ versus $1/T$ is linear in the relaxation temperature range. Using the expression

$$\sigma = \sigma_0 \exp(E_{cond}/k_B T) \qquad (2)$$

where σ_0 is the pre-exponential term, E_{cond} is the conduction activation energy, k_B is Boltzman constant and T is the absolute temperature, the

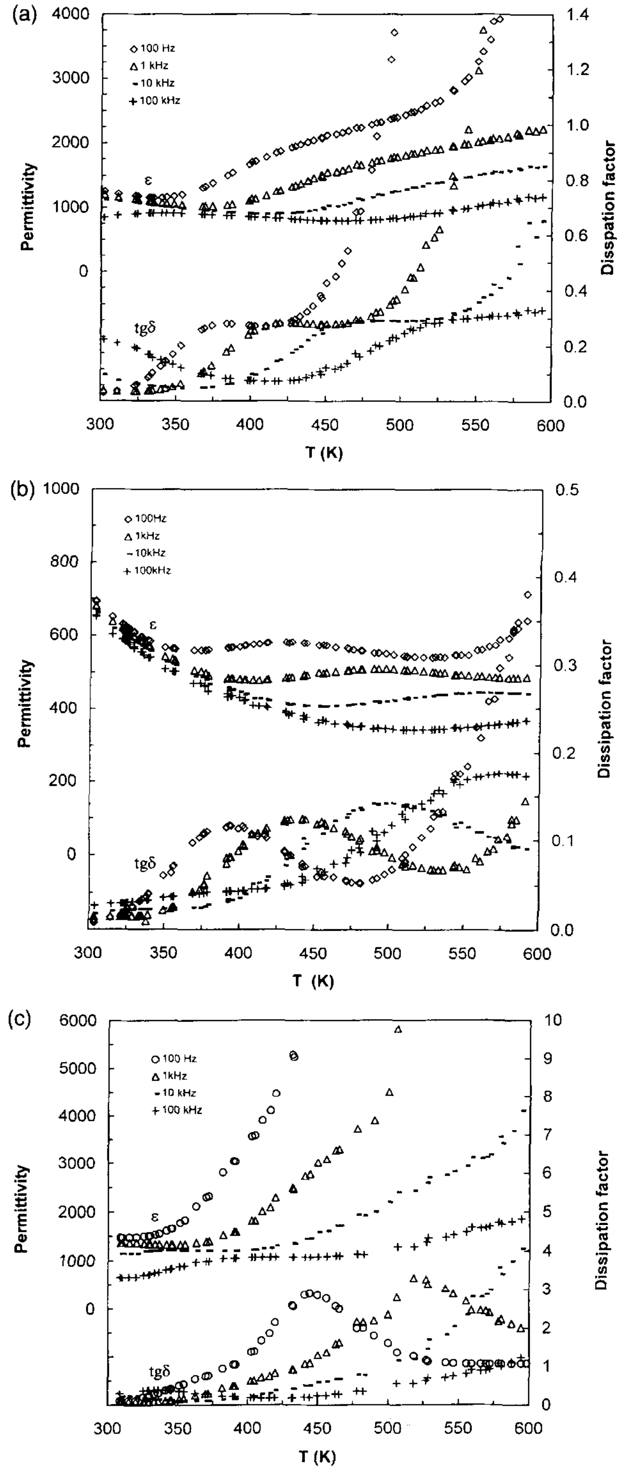

Fig. 5. Temperature and frequency dependence of permittivity and dissipation factor for the sample with $x = 0{\cdot}0533$: (a) as-sintered; (b) annealed in oxygen; (c) annealed in nitrogen.

activation energy for conduction can be calculated. The values obtained were 0·59, 0·68, 0·76 and 0·78 eV, for $x = 0{\cdot}0267$, 0·04, 0·0533 and 0·10 respectively. The values obtained are also listed in Table 1.

The dc conductivity of samples with $x = 0{\cdot}0533$ and 0·10 annealed in N_2 is shown in Fig. 10(b). It can be seen that the conductivity of the samples annealed in nitrogen is much higher than those of the as-sintered samples. The activation energy for conduction E_{cond} was calculated to be 0·64 and 0·66 eV, respectively. Comparing the activation energy for conduction before and after annealing, it can be found that the activation energy for conduction decreased by 0·08 eV after annealing in nitrogen for both samples.

4 Discussion

The study of the dielectric properties of the $(\mathrm{Sr}_{1-1\cdot5x}\mathrm{Bi}_x)\mathrm{TiO}_3$ solid solutions above room temperature (300–600 K) reveals that, in this temperature range, a set of permittivity peaks, with obvious frequency dispersion, is present.

For the Bi concentrations studied, $x = 0{\cdot}0267$, 0·04, 0·0533 and 0·10, the activation energies determined for the dielectric relaxation lie in the range $E_{\mathrm{relax}} = 0{\cdot}74 - 0{\cdot}86\ eV$, while the activation energies for conduction lie in the range $E_{\mathrm{Cond}} = 0{\cdot}59 - 0{\cdot}78\ eV$. For each composition the activation energy for conduction is always smaller than the dielectric relaxation activation energy.

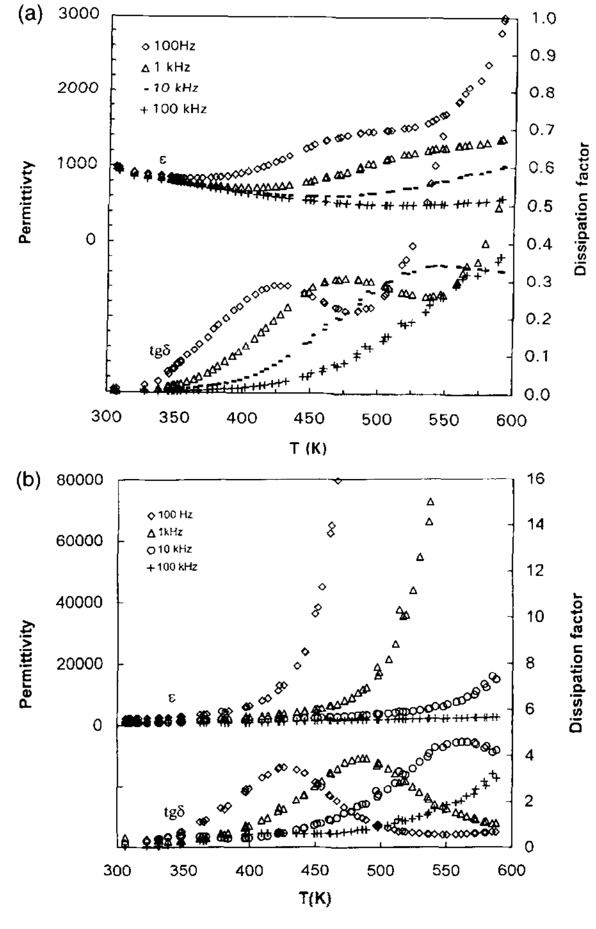

Fig. 6. Temperature and frequency dependence of permittivity and dissipation factor of the sample with $x = 0{\cdot}10$: (a) as-sintered; (b) annealed in nitrogen.

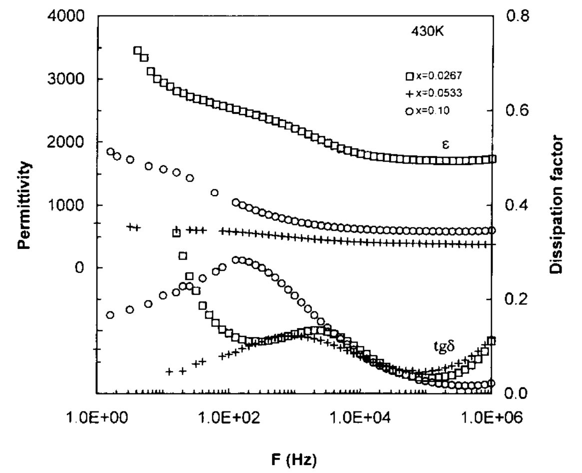

Fig. 7. Frequency dependence of permittivity and dissipation factor for $x = 0{\cdot}0267$, $0{\cdot}0533$ and $0{\cdot}10$.

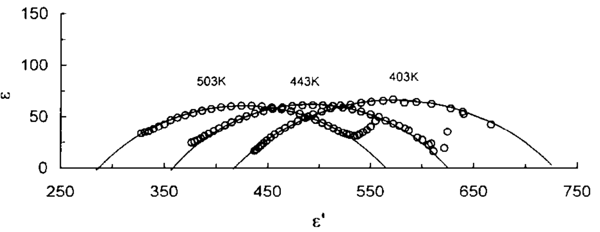

Fig. 8. Cole–Cole plot for the sample with $x = 0{\cdot}0533$ annealed in O_2.

4.1 As-sintered samples ($x = 0{\cdot}0267$–$0{\cdot}0533$)

As described in Part II of the study of the dielectric properties of the $(Sr_{1-1{\cdot}5x}Bi_x)TiO_3$ system in the low Bi concentration range, $x \le 0{\cdot}08$, the effect of the oxygen vacancies is important due to the loss of oxygen during the sintering process.[8]

The existence of oxygen vacancies will create weakly-bonded electrons that can be ionised, according to

$$V_o \rightarrow V_o^{\bullet} + e' \qquad (3)$$

$$V_o^{\bullet} \rightarrow V_o^{\bullet\bullet} + e' \qquad (4)$$

Long and Blumenthal reported that, the first-ionisation energy of the oxygen vacancy is 0·1 eV, while the second-ionisation energy is around $E_d = 1{\cdot}4$ eV.[17] Reaction (3) may, therefore, occur at room temperature or even lower temperatures. Since the energy gap of $SrTiO_3$ is $E_g = 3{\cdot}2$ eV, the energy level E_d of $V_o^{\bullet}$ is located near the middle of the band gap and at temperatures around or lower than room temperature, the second ionisation can be neglected. However, at the temperature of the present work (350–600 K), if the electrical conduction is governed by the thermal excitation of carriers from the $V_o^{\bullet}$ state to the conduction band, i.e. as described by eqn (4), one could obtain an activation energy around 0·7 eV ($E_d/2$). The values here obtained, around 0·59–0·76 eV, are not far from the values derived for pure $SrTiO_3$ and their increase may be due to distortion of the $SrTiO_3$ lattice by the increase in the concentration of the dopant.

The large values obtained for the relaxation activation energy, E_{relax}, larger than those obtained for the conduction activation energy, E_{cond}, suggest that the polarisation is of the dipole type since, if

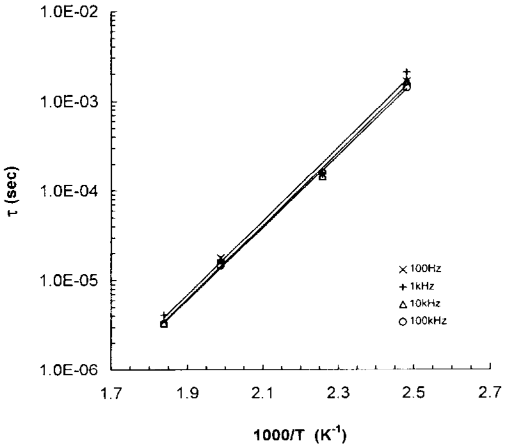

Fig. 9. Relaxation time τ versus $1/T$ curve for the as-sintered sample with $x = 0{\cdot}0533$ sample annealed in O_2.

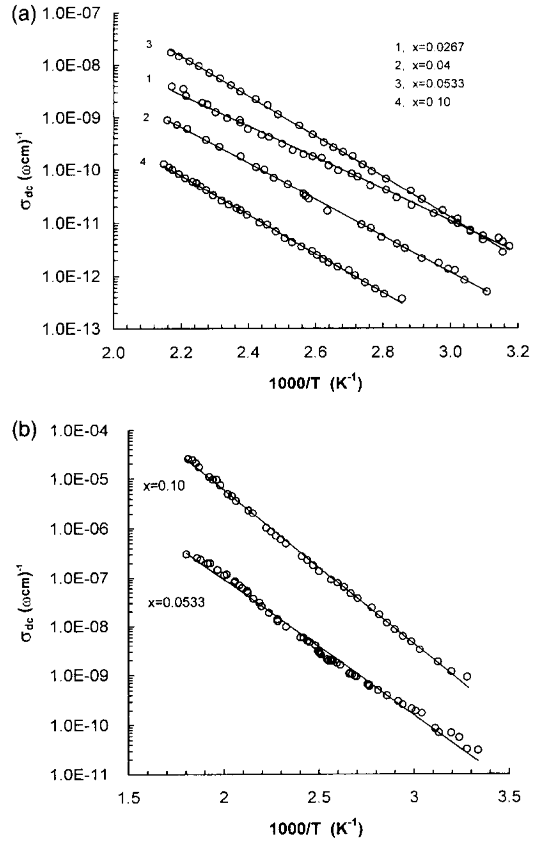

Fig. 10. (a) The dc conductivity (σ) versus $1/T$ curve for the as-sintered samples with $x = 0{\cdot}0267$, $0{\cdot}04$, $0{\cdot}0533$ and $0{\cdot}10$; (b) the dc conductivity (σ) versus $1/T$ for the samples with $x = 0{\cdot}0533$ and $x = 0{\cdot}10$ annealed in N_2.

the relaxation mechanism was governed by the trap controlled ac conduction, the values of E_{relax} were expected to be close to or less than those of E_{cond}. The dielectric relaxation can therefore be attributed to change in the dipole orientation under the influence of the external field.

In Bi doped $SrTiO_3$, several kinds of defects can be envisaged, such as $Bi_{Sr}^{\bullet}$, Ti_{Ti}' (or Ti^{3+}), $V_O^{\bullet}$, $V_O^{\bullet\bullet}$, and V_{Sr}''. Because of the Coulomb forces, the defects with positive charge can combine with defects with negative charge, forming associations of defects like (Ti_{Ti}'–$V_O^{\bullet}$), (V_{Sr}''–$2V_O^{\bullet}$), (Ti_{Ti}'–$Bi_{Sr}^{\bullet}$), (V_{Sr}''–$2Bi_{Sr}^{\bullet}$), (V_{Sr}''–$V_O^{\bullet\bullet}$) or ($2Ti_{Ti}'$–$V_O^{\bullet\bullet}$). In the temperature range of the third set of dielectric peaks dealt with in the present work, $V_O^{\bullet\bullet}$ is probably the main defect as mentioned above. Considering therefore that this set of peaks is related to oxygen vacancies, the most probable associations would be (V_{Sr}''–$V_O^{\bullet\bullet}$) and ($2Ti^{3+}$–$V_O^{\bullet\bullet}$).

The dielectric relaxation can then be related to the movement of the dipoles (V_{Sr}''–$V_O^{\bullet\bullet}$) and/or ($2Ti^{3+}$–$V_O^{\bullet\bullet}$) under the external field, i.e. small displacements of Ti^{3+}, and/or V_O, and/or V_{Sr} lead to dielectric relaxation under ac fields.[18]

Obviously, annealing in O_2 will decrease the concentration of oxygen vacancies favouring the decrease in the concentration of defect pairs and the concomitant decrease in the peak intensities. On the contrary, the N_2 annealing will favour the increase in the concentration of oxygen vacancies and the variation in peak intensity in the opposite direction.

There is however experimental evidence that points to more complicated mechanisms for the dielectric behaviour of the $(Sr_{1-1\cdot5x}Bi_x)TiO_3$ solid solutions: namely, first the values of the activation energies E_{relax} and E_{cond} obtained for the samples annealed in oxygen and nitrogen atmospheres and second the existence of the third set of permittivity peaks in the sample with $x \geq 0\cdot10$ from where the second set was absent as discussed in Part II of this study.[14]

4.2 As-sintered samples ($x = 0\cdot1$, $0\cdot133$) and the sample ($x = 0\cdot0533$) annealed in O_2

For the as-sintered samples ($x = 0\cdot1$, $0\cdot133$) and the sample ($x = 0\cdot0533$) annealed in O_2, the common features are the absence of the second set of peaks (see Part II),[15] and the existence of the third permittivity peaks. As discussed before, in these compositions, the concentration of oxygen vacancies is low, the main defects being strontium vacancies and $Bi_{Sr}^{\bullet}$ ions.

Accepting that the main defects present in these samples are strontium vacancies and $Bi_{Sr}^{\bullet}$ ions, it is reasonable to postulate that the dipole responsible for the third permittivity peaks, detected in the temperature range 300–600 K is probably correlated with V_{Sr}'', perhaps the (V_{Sr}''–$2Bi_{Sr}^{\bullet}$) association referred in Section 4.1. The dielectric relaxation can then be attributed to the small adjustment of the position of the (V_{Sr}''–$2Bi_{Sr}^{\bullet}$) under the external field, i.e. small displacement of $Bi_{Sr}^{\bullet}$, and/or V_{Sr}'', from its positions will lead to dielectric relaxation.[18]

However an alternative explanation can be thought involving oxygen vacancies. Although, as indicated by the absence of the second set of peaks in the temperature range 200–300 K, the concentration of oxygen vacancies is very low, they could still contribute, at a higher temperature (300–600 K), to the third permittivity peaks. The detailed picture would then be similar to that described in Section 4.1.

A third possibility for the appearance of the peaks in the temperature range 300–600 K could come from the well recognised easy oxidation of grain boundaries of donor doped titanates as opposed to the oxidation of the interiors of the grains. Although, as described in Part II, the interfacial polarisation (Maxwell–Wagner type polarisation) was thought not to be contributing in a significant way to the polarisation phenomena described in this set of peaks. It could be that a more detailed work proves otherwise.

4.3 Samples ($x = 0\cdot0533$ and $0\cdot1$) annealed in N_2

For the samples annealed in N_2, the concentration of oxygen vacancies can be increased, originating the second permittivity peak, similar to that described in Part II,[14] and an additional contribution for the third permittivity peak, most probably correlated with defect pairs including the oxygen vacancy. The values determined for the activation energies of dielectric relaxation and dc conduction after annealing the samples in N_2, all in good agreement (~0·63–0·66 eV), suggest the same physical nature for both conduction and dielectric relaxation. The dielectric relaxation seems therefore in this case to be related to the trap-controlled ac conduction.

5 Conclusion

A third group of relaxation peaks was observed in the $(Sr_{1-1\cdot5x}Bi_x)TiO_3$ ceramics for $x = 0\cdot0267$–$0\cdot133$.

Taking into consideration the values determined for the activation energies for dielectric relaxation and for electrical conduction, obtained for samples with different annealing treatments, it is suggested that more than one polarisation mechanisms can be responsible for the changes obtained in the dielectric permittivity peaks. It is proposed that the permittivity peaks are related to a dipole like dielectric relaxation which seems to be due to associations of defects involving oxygen vacancies for as sintered samples with x in the range 0·0267–0·0533. For the samples annealed in O_2, or with high Bi content ($x = 0{\cdot}10$ and $0{\cdot}133$), the permittivity peak seems to be related to associations of defects involving strontium vacancies. However, when the samples are annealed in nitrogen the dielectric relaxation behaviour seems to be governed by the trap-controlled ac conduction due to the second ionisation of the oxygen vacancies created by reducing atmosphere.

Acknowledgements

The authors would like to thank the financial supports of the Praxis XXI, JNICT, Portugal. One of authors (A.C.) would also thank Zhejiang University, People's Republic of China, for permitting his leave and work in the University of Aveiro.

References

1. Waser, R., Electrochemical boundary conditions for resistance degradation of doped alkaline–earth titanates. *J. Am. Ceram. Soc.*, 1989, **72**, 2234–2240.
2. Frederikse, H. P. R., Thurber, W. R. and Hosler, W. R., Electronic transport in Strontium titanate. *Phys. Rev.*, 1964, **134**, A442–445.
3. Viana, R., Lunkenheimer, P., Hemberger, J., Böhmer, R. and Loidl, A., Dielectric spectroscopy in $SrTiO_3$. *Phys. Rev. B*, 1994, **50**, 601–604.
4. Blance, J. and Staebler, D. L., , Electrocoloration in $SrTiO_3$: vacancy drift and oxidation-reduction of transition metals. *Phys. Rev. B*, 1971, **4**, 3548–3557.
5. Waser, R., Bulk conductivity and defect chemistry of acceptor-doped strontium titanate in the quenched state. *J. Am. Ceram. Soc.*, 1991, **74**, 1934–1940.
6. Denk, I., Münch, W. and Maier, J., Partial conductivities in $SrTiO_3$: bulk polarisation experiments, oxygen concentration cell measurement, and defect-chemical modelling. *J. Am. Ceram. Soc.*, 1995, **78**, 3265–3272.
7. Moos, R., Gnudi, A. and Härdtl, H., Thermopower of $Sr_{1-x}La_xTiO_3$ ceramics. *J. Appl. Phys.*, 1995, **78**, 5042–5047.
8. Moos, R. and Härdtl, K. H., Electronic transport properties of $Sr_{1-x}La_xTiO_3$ ceramics. *J. Appl. Phys.*, 1996, **80**, 393–400.
9. Nishigaki, S., Murano, K. and Ohkoshi, A., Dielectric properties of ceramics in the system $(Sr_{0.50}Pb_{0.25}Ca_{0.25})TiO_3$–$Bi_2O_3{\cdot}3TiO_2$ and their application in a high-voltage capacitor. *J. Am. Ceram. Soc.*, 1982, **65**, 554–560.
10. Burn, I. and Neirman, S., Dielectric properties of donor-doped polycrystalline $SrTiO_3$. *J. Mater. Sci.*, 1982, **17**, 3510–3524, and the references therein.
11. Chen, A., Zhi, Y., Zhi, J., Vilarinho, P. M. and Baptista, J. L., Dielectric properties of $(Sr_{0.76}Bi_{0.16})TiO_3$–$PbTiO_3$ ceramics. *Bol. Soc. Esp. Ceram. y Vidrio* 1998, **37**, 235–238.
12. Skanavi, G. I., Ksendzov, I. M., Trigubenko, V. A. and Prokhvatilov, V. G., Relaxation polarisation and losses in *non-ferroelectric* dielectrics with high dielectric constants. *Sov. Phys. JETP*, 1958, **6**, 250–259.
13. Gubkin, A. N., Kashtanova, A. M. and Skanavi, G. I., Dielectric properties of strontium bismuth titanates at low temperature. *Soviet Phys.: Solid State*, 1961, **3**, 807–813.
14. Zhi, Y., Chen, A., Vilarinho, P. M., Mantas, P. Q. and Baptista, J. L., Dielectric relaxation behaviour of Bi:Sr-TiO_3: II. Influence of heat treatment on dielectric properties. *Journal of the European Ceramic Society*, in press.
15. Zhi, Y., Chen, A., Vilarinho, P. M., Mantas, P. Q. and Baptista, J. L., Dielectric relaxation behaviour of Bi:Sr-TiO_3: I. The low temperature permittivity peak. *Journal of the European Ceramic Society*, in press.
16. Cole, K. S. and Cole, R. H., Dispersion and absorption in dielectrics I. Alternating current characteristics. *J. Chem. Phys.*, 1941, **9**, 341–351.
17. Long, S. A. and Blumenthal, R. N., Ti-rich nonstoichiometric $BaTiO_3$: II. Analysis of defect structure. *J. Am. Ceram. Soc.*, 1971, **54**, 577–583.
18. Jonscher, A. K., *Dielectric Relaxation in Solids*. Chelsea Dielectrics Press, London, 1983, p. 326.